JOURNAL OF THERMOPHYSICS AND HEAT TRANSFER
Vol. 14, No. 3, July–September 2000

Thermal Characterization of Aerospace Structures

A. R. Hanuska*
E. I. DuPont, Inc., Wilmington, Delaware 19880-0356
E. P. Scott†
University of Utah, Salt Lake City, Utah 84112-9208
and
K. Daryabeigi‡
NASA Langley Research Center, Hampton, Virginia 23681

Predicting the thermal performance of complex aerospace structures requires accurate knowledge of the thermal properties associated with the structure. It is desired, in this case, to measure the in situ properties of a complex as-built structure, not only to capture the thermal properties of each component but also to capture interaction of components in the as-built structure. The overall goal of this study was, therefore, to develop and implement a nondestructive methodology to estimate the thermal properties associated with a complex aerospace structure. The structure considered was an outer wing subcomponent design for the high-speed civil transport made from four different materials, including a honeycomb blanket. The thermal properties sought included both effective and individual material through-the-thickness thermal conductivities and volumetric heat capacities (product of density and specific heat) and the in-plane thermal conductivities of each material in the structure. In the estimation procedure an objective function containing both theoretical and experimental temperature histories was minimized using a genetic algorithm. One-dimensional experiments were implemented to estimate the through-the-thickness thermal conductivities and volumetric heat capacities, and two-dimensional experiments were conducted to estimate the in-plane conductivities. These properties were successfully estimated despite the high degree of correlation and low sensitivity evident for many of the properties.

Nomenclature

C = volumetric heat capacity, J/m^3 · K
CI = confidence interval
k = thermal conductivity, W/m · K
N = total number of experiments
n_p = number of parameters estimated
S = sum-of-squares function
s = standard deviation
$\boldsymbol{T}$ = calculated temperature vector
X = sensitivity coefficients
$\boldsymbol{X}$ = sensitivity vector
$\boldsymbol{Y}$ = measured temperature vector
β = unknown thermal properties vector
Δx = element width (one-dimensional model)
σ = predicted uncertainty

Subscripts

CS = composite skin
eff = effective
FS = facesheet
HC = honeycomb blanket
PT = predicted temperature
s = sensitivity
T = temperature
TT = torque tube
v = variance
βi = ith parameter
$\perp$ = through-the-thickness (thermal conductivity)
$=$ = in-plane (thermal conductivity)

Superscript

$+$ = normalized

Introduction

PREDICTING the performance of complex structures exposed to harsh thermal environments is a crucial issue in many of today's aerospace and space designs. To predict the thermal stresses a structure might be exposed to, the thermal properties of each material in the design of the structure need to be known.

The goal of this research was to determine nondestructively the thermal properties associated with a complex structure, namely an outer wing subcomponent (OWS) design for the high-speed civil transport (HSCT). This structure is made from high strength-to-weight ratio materials including honeycomb blankets and carbon-fiber/epoxy-matrix composites. The specific objectives for this work were to formulate an overall strategy for the estimation procedure, develop a mathematical thermal model of the OWS, design and conduct experiments to generate the required data for the estimation procedure, and estimate the desired thermal properties.

The estimation strategy involved the formulation of a least-squares objective function containing both calculated temperatures from the mathematical model and experimental temperature data. A genetic algorithm developed previously[1,2] was used to minimize the objective function to estimate the desired properties.

Background

Both steady-state and non-steady-state techniques have been developed to determine thermal properties for independent materials.[3,4] However, in complex structures it is not only desired to determine the properties of each material, but it is also desired to capture the interactions of the as-built structure (e.g., including contact resistances at the interfaces); therefore, other approaches were sought.

The nonlinear least-squares method allows for the simultaneous estimation of thermal properties in a transient analysis. Here, an objective function formed from theoretical and experimental temperature data is minimized to determine the desired thermal properties.

Received 28 May 1999; revision received 21 October 1999; accepted for publication 22 October 1999.

*Technical Engineer, DuPont Central Research and Development, Chemical Science and Engineering.
†Associate Professor, Department of Mechanical Engineering.
‡Aerospace Engineer, Thermal Structures Branch.

One common minimization method is the Gauss technique, which has been used to estimate the thermal properties of composites.[5–9] This technique is a derivative-based method that can exhibit slow or nonconvergence in cases of extremely flat objective functions where correlation between properties is present and in cases where several local minima are present. Copenhaver et al.[10] circumvented this problem through the use of a penalty function technique, whereas others have adopted a different strategy through the use of genetic algorithms (GAs).[2]

GAs, as the name implies, are based on natural selection mechanisms and the Darwinian principle of the survival of the fittest. Here, each unknown property is associated with a gene, and a chromosome is a combination of genes representing one specific solution or, in this case, a set of estimated properties. Developed in 1975, this method has seen limited use in thermal applications. Raudensky et al.[11] used GAs to solve an inverse heat conduction problem, whereas Fabbri[12] applied GAs to the thermal design of finned surfaces. Most recently, GAs have been applied to the optimization of experiments and subsequent estimation of thermal and radiative properties of composite and insulative materials.[1,2] This technique proved to be successful, despite a high degree of correlation between the thermal properties estimated. Because of the robustness of this method, it was chosen for use in this study.

OWS Test Specimen

The OWS design investigated in this study was developed to determine the feasibility of using unitized composite construction in the wing of the HSCT. The OWS was built from several different materials as shown by the numbered components in Fig. 1a; the dimensions are shown in Fig. 1b. The entire structure was tapered in two dimensions, such that it formed trapezoids along three planes. The core of the OWS sample (1) consisted of three torque tubes constructed of six plies of T300/954-2A eight-harness satin cloth prepreg. On either side of the tubes were the upper and lower composite skins (2), which were fabricated from 28 plies of IM/954-2A composite. Honeycomb blankets (3) were placed on either side of the skins. These 25.4-mm high 321 stainless-steel foil structures are used for their high strength-to-weight ratio. Finally upper and lower facesheets (4) assembled with 24 plies of IM7/PETI-5 composite prepreg were placed on the outermost surfaces. The edges of the OWS sample were protected with closeouts and edge channels (5-6) fabricated from T300/954-2A 8 composite prepreg.

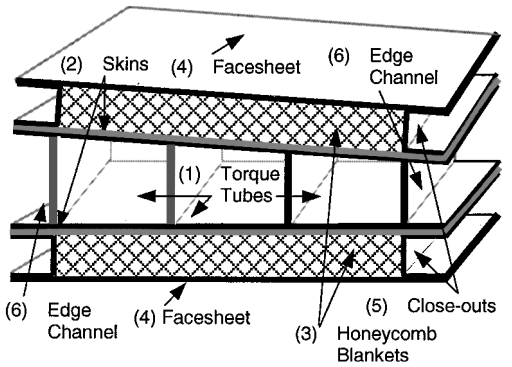

a) Front view

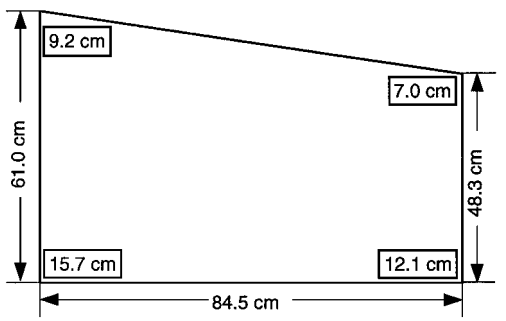

b) Top view: dimensions (□ indicates thickness at corners)

Fig. 1 OWS test specimen (not to scale).

Estimation Strategy

The estimation strategy was based on the minimization of an objective function formulated from experimental and calculated temperature data. The experimental data were obtained from transient experiments in which the thermal response of the OWS to an applied heat flux was recorded. The calculated temperatures were obtained from a mathematical model designed to simulate the experiments. This objective function is described mathematically as

$$S = [\boldsymbol{Y} - \boldsymbol{T}(\beta)]^T [\boldsymbol{Y} - \boldsymbol{T}(\beta)] \tag{1}$$

Here, the calculated temperatures in $\boldsymbol{T}(\beta)$ were determined at the corresponding times and locations as the measured temperatures in $\boldsymbol{Y}$. $\boldsymbol{T}(\beta)$ is a function of β, which is a vector of the unknown thermal properties inherent in the mathematical model. The desired β, therefore, contains the thermal properties that minimize the objective function.

Thus, in addition to experimental studies and a mathematical model, an optimization procedure was needed to minimize Eq. (1). All three of these facets are discussed in the following sections. The mathematical and experimental studies were integrated, i.e., the mathematical models were first used to design the experiments, and then the practical limitations of the experiments were incorporated back into the models.

Mathematical Models

The OWS structure was analyzed, using three different models with increasing complexity. First a one-dimensional model was developed from which the effective thermal properties through the thickness of the model $k_{\perp_{\text{eff}}}$ and C_{eff} were determined. The next model again considered one-dimensional heat transfer through the thickness, but in this case the details of the different structural components were considered. Here, the thermal properties of interest were the through-the-thickness thermal conductivities and the volumetric heat capacities of each material (i.e., $k_{\perp_{\text{FS}}}$, $k_{\perp_{\text{HC}}}$, $k_{\perp_{\text{CS}}}$, $k_{\perp_{\text{TT}}}$, C_{FS}, C_{HC}, C_{CS}, and C_{TT}). In the last model two-dimensional heat transfer was considered so that the in-plane thermal conductivities could also be investigated, namely, $k_{=\text{FS}}$, $k_{=\text{HC}}$, $k_{=\text{CS}}$, and $k_{=\text{TT}}$.

To simultaneously estimate k and C independently, it was necessary to apply a known heat flux at one boundary. This allowed for the introduction of Fourier's law as a boundary condition with thermal conductivity independent of volumetric heat capacity. A constant temperature condition was initially assumed at the opposite boundary. Each of the models was solved numerically using a commercial general finite element code.[13] A desired feature of this code was that user-developed subprograms (e.g., the GA) could be incorporated with the prepackaged programs (e.g., the conduction heat transfer solver).

Effective One-Dimensional Model

In the effective one-dimensional model the individual components were lumped together, such that only the effective properties were of interest. This model provided useful information on the implementation of the estimation procedure and on the overall thermal performance of the test specimen. Because the heater was applied over the entire top surface of the sample, transient heat conduction was considered through the thickness over the area of one element with a width of Δx, with a known heat flux at one boundary and a known temperature at the opposite boundary. In this model the effective thermal properties were assumed to be constant because of the small temperature change (< 10 K) through the thickness of the OWS during each experiment, and the thickness of the sample was assumed to be equal to the average thickness of the trapezoidal physical model.

In the experimental setup a heat sink was used to simulate a constant temperature boundary condition at the lower boundary. However, thermocouples placed at this boundary indicated that this

temperature varied slightly. Therefore, a specified (rather than constant) temperature boundary condition was implemented using these measurements. A question also arose on how to model the heated surface because the exact value of the heat flux into the material was needed in the model. As described later in the experimental procedures, insulation was placed on the top surface of the heater, and the total power input into the heater was recorded. Because it was found that some of the heat was indeed lost through the insulation, the model was modified to include the insulation and convective heat transfer at the top surface through an effective resistance at the boundary.

Detailed One-Dimensional Model

The detailed one-dimensional model differed from the effective model in that heat transfer though each individual subcomponent was considered in the detailed model in order to estimate the thermal properties of the individual materials. In addition, because the physical model was essentially symmetric through the thickness, only the top portion of the physical model was considered. Thus, as shown in Fig. 2, the model included only the top layer of the torque tube. As illustrated in the experimental section, temperature measurements at the inner top surface of the torque tubes were used (with interpolation) as one boundary condition for the model. Finally, the thickness of the sample and the heat flux boundary condition were treated as they were in the effective model: the average thickness of the physical sample was used, and the insulation and convection at the heated surface were included in the model.

Detailed Two-Dimensional Model

The detailed two-dimensional model is shown in Fig. 3. This model differed from the previous models primarily in that two-dimensional heat transfer was considered by applying the heat flux to only one-half of the top surface, and the width of the model was now equal to the width of the actual sample. The top boundary was again modeled with insulation and convection, and only the top portion of the physical sample was considered. Experimental temperature data were used as the lower boundary condition with linear interpolation. Finally, an insulative boundary condition was assumed at the sides.

Sensitivity Study

A sensitivity study can be used to provide important information on the thermal properties to be estimated, and it supplies the basis for the optimization of the experimental design. The sensitivity study was based on the calculation of the normalized sensitivity coefficients defined as

$$X_i^+ = \beta_i \frac{\partial T}{\partial \beta_i} \tag{2}$$

Inspection of these coefficients can provide insight on the information available for property estimation and the degree of correlation between properties. The magnitude of X_i^+ provides an indication of how much information is available for the estimation of a particular property; values greater than 10% the maximum experimental temperature rise are desired. On the other hand, near correlation can at times result in nonconvergence in the simultaneous estimation of different properties. Sensitivity curves of similar shapes can be a visual indication of correlation problems.

Once the sensitivity coefficients are found, they can also be used to determine the user-defined parameters which optimized the experimental design. In this case the duration of the applied heat flux and the location of the temperature sensors [used in Eq. (1)] were the primary parameters of interest. It is desired to design the experiment with maximum sensitivity. One criterion to achieve this is commonly called the D criterion. Here the determinant of the $\boldsymbol{X}^T\boldsymbol{X}$ matrix is maximized, where $\boldsymbol{X}$ is the sensitivity vector that contains the (dimensional) sensitivity coefficients X_i. Therefore, an optimization procedure was needed to determine the experimental parameters of interest. Here, the same optimization procedure used to estimate the thermal properties was also used to optimize the experiment.

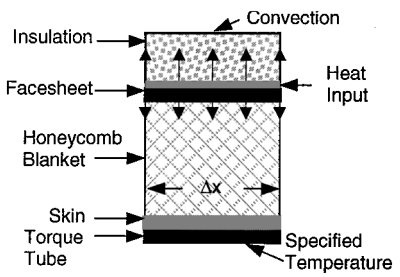

Fig. 2 Detailed one-dimensional model (not to scale).

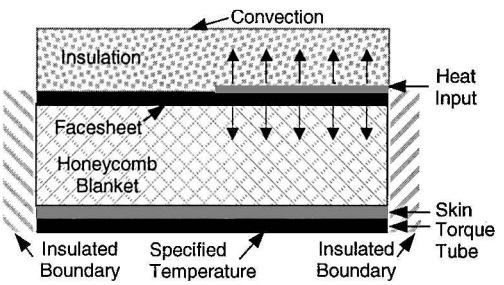

Fig. 3 Two-dimensional model (not to scale).

Confidence Intervals

Whenever results are obtained from experimental data with inherent uncertainties, it is crucial to determine the uncertainties of the results (i.e., thermal properties) derived from that data. Therefore, 95% confidence intervals were calculated for each estimated property. The confidence intervals for the properties estimated from each experiment were calculated from the sensitivity coefficients of that property and the uncertainty of the independent variables.[14] Here, assuming an unbiased model with measurements of temperature only, we can write the uncertainty of a given property β_i for a particular experiment j as

$$U_{j,\beta_i,95\%} = \left(\frac{\partial \beta_i}{\partial T}\right) s_{T_i} t_{95\%,\nu_j} \tag{3}$$

where the Student's t multiplier is found for ν_j degrees of freedom at the 95% confidence level. Note that the X_i^+s change as a function of time and location; therefore, the $\partial\beta_i/\partial T$ values are not constant. Thus, these values were estimated at a given location as the inverse of the time-averaged sensitivity coefficient as shown next:

$$\left(\frac{\partial \beta_i}{\partial T}\right) \approx \left(\frac{1}{t_n}\int_0^t X_i \, \mathrm{d}t\right)^{-1} \tag{4}$$

Given $U_{j,\beta_i,95\%}$, the confidence intervals of the mean estimates from all of the experiments can then be found from[1]

$$\overline{CI}_{s,\beta_i,0.95} = \frac{t_{95\%,N-1}}{N}\sqrt{\sum_{i=1}^{N}\left(\left(\frac{\partial \beta_i}{\partial T}\right)s_{T_i}\right)^2} \tag{5}$$

These confidence intervals are referred to as sensitivity confidence intervals.

Commonly, confidence intervals are calculated from the variance of the estimated parameters from multiple runs without any sensitivity information. Thus, the variance confidence intervals are defined as

$$\overline{CI}_{v,\beta_i,0.95} = \frac{t_{95\%,N-1} s_{\beta_i}}{\sqrt{N}} \tag{6}$$

Because Eq. (5) contains both sensitivity and statistical information, these confidence intervals will often tend to be greater than those calculated using Eq. (6).

Experimental Methodology

All experiments were built and conducted at NASA Langley Research Center in Hampton, Virginia. The OWS test specimen was fabricated by an independent supplier. The construction of the experimental setup and the procedures used in the experiments are described in the following subsections.

Experimental Setup

Two experimental setups were used: a one-dimensional setup and a two-dimensional setup. In each setup one surface was held at a constant temperature, a heat flux was applied at the opposite surface, and the remaining sides were insulated. The same sample was used in both setups, which were the same except for the size of heater used to impose the heat flux. In the one-dimensional case the heater covered the entire top surface of the sample, whereas the heater covered only half the surface in the two-dimensional setup. Experiments were run at three different temperatures (295 K, 375 K, 445 K) with up to six experiments at each temperature setting to ensure repeatability.

In each setup an aluminum heat sink was used to simulate a constant temperature boundary condition. The OWS sample was placed on top of the heat sink, and thermal grease was used between the heat sink and the sample to reduce the thermal contact resistance at the interface.

Temperature was measured using AWG 30 Type K thermocouples. Fifty-four thermocouples were used for the one-dimensional setup, whereas a total of 81 thermocouples were used in the two-dimensional case. In the one-dimensional case 16 thermocouples were placed on the top surface of the sample next to the heater in a regular grid pattern, and 20 were placed on the bottom surface at the constant temperature boundary condition. The remaining 18 thermocouples were bonded to the top, side, and bottom inner tube surfaces. The thermocouples were placed in a similar manner in the two-dimensional case, with the exception that additional thermocouples were placed at the top, inner, and bottom surfaces under the heater closest to the outer edge of the OWS. As a result of the optimization of experiment, the temperature measurements were found to be the most sensitive at these locations. Nominal calibration curves were used for the thermocouples. (Note that the temperature difference rather than absolute temperature was of primary importance in the estimation procedure.) The standard deviations of the temperature measurements with no heating for the one- and two-dimensional experiments were approximately 0.02 and 0.09 K, respectively.

The imposed heat flux was supplied by thin, flexible silicone rubber fiberglass insulated heaters. As already mentioned, two heaters were used: a heater fitting the exact dimensions of the upper surface of the sample was used in the one-dimensional case, whereas the other was fabricated to cover only half of the surface. Each heater was bonded on one side to a thin copper sheet to ensure a uniform heating pattern. This was verified using a thermal imaging system before and after the copper sheet was applied. The heating pattern was clearly visible without the copper sheet, but unobservable (i.e., uniform) with the sheet included. The heaters were placed on the top surface of the OWS test specimen using thermal grease to ensure good contact between the sample and the heater.

The voltage and current supplied to the heater were read using multimeters, and the resulting signals were recorded by a data acquisition system. The voltage readings from the thermocouples were also read into the data acquisition system, where internal software was used to convert the mvolt readings into temperature using a calibration curve.

Ceramic insulation was used on top of the heated surface in both one- and two-dimensional setups. This was done to reduce heat loss from the top of this surface. Thermocouple measurements placed on top of this surface indicated that some heat was indeed lost from the top. As a result, the insulation and the convective boundary condition were incorporated into the model, as already discussed. In addition, the same ceramic insulation was placed around all four sides of the sample to provide an insulated boundary condition. (Because the edges were not heated, the insulation proved to be sufficient here.)

To determine the variability of the thermal properties as functions of temperature, an oven was built to provide the necessary ambient conditions for the sample. (Because of the sample's large size, economical commercial ovens were not available for this purpose.) The frame of the oven was constructed of steel U channels, and the walls were constructed of ceramic insulation boards wrapped in aluminum foil and mounted to plywood boards for support. The aluminum heat sink was set in a sliding tray at the bottom of the oven. Inlet and outlet air duct holes were placed at the bottom and top respectively of one side wall of the oven. Air was supplied to the oven by a blower with a temperature-controlled heating unit. Thus, heat in the oven was supplied by convection, and the temperature was controlled by the blower unit.

Experimental Procedures

The experimental setup was first assembled as already described. After the setup was in place and the heater and thermocouple leads were connected to the data acquisition system, the temperature controller for the blower was set at the desired testing temperature. The temperature within the oven and sample were monitored (but not recorded) over time (e.g., several hours) to ensure thermal equilibrium. Once thermal equilibrium was established, the data acquisition system was activated. A few temperature data were recorded prior to activating the heater to determine the variance in the temperature readings and the off sets between thermocouple channels. The heater was then activated to approximately 20 W/m^2 for a predetermined optimal heating time. (This resulted in a temperature rise of approximately 5 K at the surface of the sample.) The data acquisition system remained activated after heating, recording data at 15-s intervals, until the OWS sample cooled to the equilibrium conditions at the initial oven temperature. At this time the data acquisition system was turned off, and the experiment was complete.

Optimization Procedure

The optimization procedure was implemented using mathematical and experimental data. The optimization procedure and its implementation are described next.

GA

The objective function shown in Eq. (1) was minimized using a GA. The specific GA used here is called an extended elitist genetic algorithm (EEGA) and is described in detail by Garcia and Scott.[1] An overview is provided next.

The basic steps in the EEGA first involve the generation of an elitist initial population that is created from a number of initial random populations. Each random population contains a number of different chromosomes, which are different estimates of the vector β randomly selected from predetermined ranges for each of the unknown properties contained in β. Once these populations have been created, they are ranked in ascending order, according to the value of the objective function obtained from Eq. (1). A preselected number of the top-ranked chromosomes from each initial population form the initial elitist population.

Once the initial elitist population has been formed, the chromosomes are ranked according to their objective function S, and a roulette-wheel selection methodology is used to select the best parent chromosomes for breeding. Breeding is the formation of new chromosomes β from a combination of two parent chromosomes. The resulting population of children is then combined with the parent population, and the combined population is reranked. A specified number of new chromosomes are then added to the population to introduce new blood (i.e., new estimates) to help prevent convergence on a nonoptimal chromosome.

The process was repeated until a convergence criterion was met. Because the original EEGA did not have a stopping criterion, a new criterion was implemented in this study. Here, convergence was assumed if the average of the top 20 objective functions S changed less than 1% for three generations.

Implementation of the Estimation Procedure

Once the mathematical models were developed and the experiments were completed, the optimization procedure just described was implemented for the estimation of the desired unknown thermal properties. The procedure was first implemented using the one-dimensional effective model and the experimental data from the one-dimensional experimental setup. The unknown properties here were $k_{\perp_{\text{eff}}}$ and C_{eff}. (Thus, the vector β contained two coefficients.) Data from the thermocouples located next to the heater were (spatially) averaged at each measurement time step to form the vector $\boldsymbol{Y}$, and the one-dimensional effective mathematical model was used to provide the calculated temperature vector $\boldsymbol{T}$ in Eq. (1). The estimation procedure was then applied to the detailed one-dimensional model in a similar fashion, except that β contained eight coefficients, namely, $k_{\perp_{\text{FS}}}$, $k_{\perp_{\text{HC}}}$, $k_{\perp_{\text{CS}}}$, $k_{\perp_{\text{TT}}}$, C_{FS}, C_{HC}, C_{CS}, and C_{TT}. Finally, the process was implemented using the two-dimensional model and data from the two-dimensional experimental setup. Here, the estimates from the one-dimensional detailed experiment were used in the model so that only the in-plane thermal conductivities were the properties of interest; thus, β contained four coefficients: $k_{=_{\text{FS}}}$, $k_{=_{\text{HC}}}$, $k_{=_{\text{CS}}}$, and $k_{=_{\text{TT}}}$.

The GA required the specification of the initial and elitist populations, the number of new chromosomes added in each generation, and the initial parameter ranges for each of the parameters estimated. In this study five initial populations of 50 each (i.e., 250 total) were used to form the initial elitist parent population of 50 (i.e., only the top 50 ranking objective functions were retained). At each generation 10 new chromosomes were randomly generated and used to replace the bottom 10 ranking chromosomes (according to their objective functions). Previous knowledge should be used as much as possible in determining the initial parameter ranges. Note that, in general, the number of generations required will be reduced as the initial ranges are narrowed, thus reducing computation time; however, care should be taken such that the ranges are not reduced to the point that the optimum solution is excluded. Thus, based on properties of similar materials, the following approximate parameter ranges were used: $k_{\perp}$ (all materials)—0.01 to 10 W/m · K; $k_{=}$ (all materials)—0.01 to 100 W/m · K; and C (all materials)—0.01 to 10 MW/m^3 · K.

Results and Discussion

Sensitivity Analysis

The sensitivity analysis involved both calculation of the sensitivity coefficients and the subsequent optimization of several experimental parameters.

Sensitivity Coefficients

The sensitivity coefficients were first calculated for each estimated property as a function of time. The normalized sensitivity coefficients for $k_{\perp}$, C, and $k_{=}$ for each material (with units of K) are shown in Figs. 4–6, respectively. (Note that order of magnitude estimates of the properties were used to normalize the sensitivity coefficients; therefore, the sensitivity coefficients are evaluated on an order-of-magnitude basis only.) From Figs. 4 and 5 the sensitivities of $k_{\perp}$ and C for the honeycomb blanket are significantly greater than the sensitivities for the other materials, indicating that there is more information for the estimation of the honeycomb properties than for the others. Also, note the similarity in the shapes of the curves for $k_{=_{\text{CS}}}$ and $k_{=_{\text{TT}}}$ and for C_{CS} and C_{TT} in particular. This indicates correlation between the properties. Near correlation infers that although independent estimates can be obtained it can be difficult, particularly if gradient minimization methods are used.

Note that in Fig. 6 the sensitivity for $k_{=}$ of the honeycomb blanket dominates, whereas the sensitivity for the other materials is quite small, suggesting that very little information is available for the estimation of these material properties.

Optimization of the Experiment

The experimental parameters optimized were the total heating time for both one- and two-dimensional setups and the sensor location for the two-dimensional setup. (Based on earlier experience, the optimal sensor location for the one-dimensional setup is at the heated surface.) Using the genetic algorithm to maximize the determinant of the $\boldsymbol{X}^T\boldsymbol{X}$ matrix, the optimum heating times were found to be 264 min for the one-dimensional case and 284 min for the two-dimensional set up. These were the heating times and not the total experimental times. The total experimental times were set at twice the heating time. The optimum sensor location for the two-dimensional setup was at the edge of the sample under the heated surface.

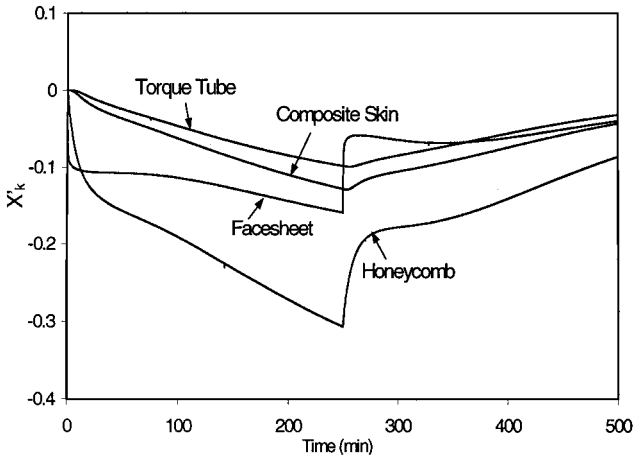

Fig. 4 Normalized sensitivity coefficients (K) for through-the-thickness thermal conductivity.

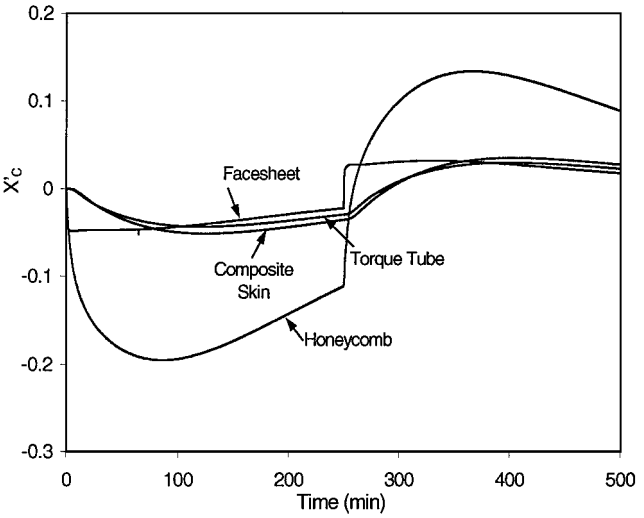

Fig. 5 Normalized sensitivity coefficients (K) for volumetric heat capacity.

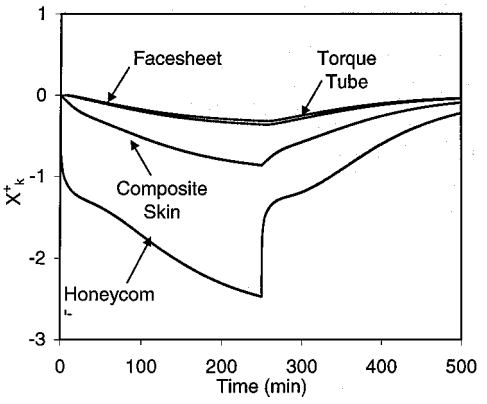

Fig. 6 Normalized sensitivity coefficients (K) for in-plane thermal conductivity.

Table 1 Estimates of $k_{\perp_{eff}}$ and C_{eff} from the one-dimensional effective model

T, K	$k_{\perp_{eff}}$, W/m · K	C_{eff}, MJ/m^3 · K
295	0.28 ± 0.21[a]	4.31 ± 6.93[a]
	± 0.19[b]	± 1.41[b]
375	0.49 ± 0.08[a]	4.38 ± 1.41[a]
	± 0.02[b]	± 0.32[b]
445	0.59 ± 0.08[a]	4.55 ± 1.30[a]
	± 0.06[b]	± 0.47[b]

[a] CI_s from Eq. (5). [b] CI_v from Eq. (6).

Estimation of Thermal Properties

The thermal properties were estimated using data from the two different experimental setups and the three different models. (Data from the one-dimensional experimental setup were used with both the effective and detailed one-dimensional models.) These results are presented next.

Effective One-Dimensional Model

The effective thermal conductivities and volumetric specific heats were estimated using data from three experiments at 295 K and six experiments each at 375 and 445 K. The average estimates for each temperature and corresponding 95% confidence intervals calculated from Eqs. (5) and (6) are shown in Table 1. The estimates for effective thermal conductivity indicate some temperature dependence, whereas the estimates for the effective volumetric heat capacity are relatively constant. A Student's t means test was performed, and the results confirmed that the mean estimates for $k_{\perp_{eff}}$ at different temperatures differed significantly, whereas those for C_{eff} did not. The estimates for both $k_{\perp_{eff}}$ and C_{eff} at room temperature (295 K) had the highest confidence intervals. This is a combined result of higher variability in the estimates for each repetition and fewer repetitions at that temperature. Also, the sensitivity and the variance confidence intervals for $k_{\perp_{eff}}$ were relatively close, whereas the CI_s values were much larger than the CI_v values for specific heat. This is a result of the higher sensitivity for $k_{\perp_{eff}}$ than for C_{eff}.

Detailed One-Dimensional Model

The thermal conductivities and volumetric specific heats of the individual materials in the OWS were also estimated using data at the three different temperatures from the one-dimensional experimental setup. The average estimates for the through-the-thickness thermal conductivity and the volumetric heat capacity for each temperature and 95% confidence intervals from Eqs. (5) and (6) are shown in Table 2.

The difference between the two methods used in calculating the confidence intervals is quite apparent in this case. The effect of including sensitivity information in the confidence intervals resulted in some cases where the sensitivity confidence intervals were several orders of magnitude greater than the variance confidence intervals, especially for C, which has the implication that, in some cases, despite the lack of information for the estimation procedure relatively consistent estimates were obtained, as indicated by CI_v. In looking at the estimates of $k_\perp$, note that the estimates of $k_{\perp_{HC}}$ have the smallest confidence intervals and are very close to the $k_{\perp_{eff}}$ values at the corresponding temperatures. This suggests that the honeycomb blanket is the most significant thermal material in the OWS thermal model. (Note that the effective model also includes the air within the torque tubes.) Also, the sensitivity confidence intervals in particular for the other materials are relatively high. The reason for this can be seen by looking at Fig. 4. The sensitivity coefficients for $k_{\perp_{HC}}$ are much higher than for the other materials, indicating that there is more information available from the data for the estimation of this property than for the other properties. This result was expected simply because of the relative thinness of the other materials relative to the honeycomb layer. These results have several implications. Firstly, for this type of heating load (at the surface), it is most important to accurately know $k_{\perp_{HC}}$ to predict the temperature response of the OWS. (As a reminder, this is the overall goal: to provide properties that can be used in thermal models for thermal stress analyses.) In other words, a high degree of accuracy in the estimates for $k_{\perp_{FS}}$, $k_{\perp_{CS}}$, and $k_{\perp_{TT}}$ is not needed for the thermal model, and perhaps the model could be simplified using lumped capacitance. In this case thermal stresses can be neglected because of the negligible temperature gradient. On the other hand, if more accuracy is sought for these properties (say for a different type of heating load or a different OWS design), then perhaps the experiment could be further optimized to maximize the sensitivity of these properties. For example, this might be achieved using thermal sensors embedded within the structure during fabrication. The generally higher confidence intervals for the 295 K case is again a result of fewer runs at this temperature and higher variability within the estimates at this temperature.

When looking at the estimates for the volumetric heat capacity in Table 2, the confidence intervals are relatively higher than those for $k_\perp$. Comparing the normalized sensitivity coefficients for C in Fig. 5 with those for $k_\perp$ in Fig. 4 reveals that the sensitivity of the volumetric heat capacities were all less than that for $k_{\perp_{HC}}$. Therefore, there was less information available for the estimation of C and hence the higher confidence intervals. This is particularly true for C_{CS}, C_{TT}, and C_{FS}, which have very low sensitivities and consequently high CI_s values. There was, however, more information for the estimation of C_{HC} than for the other through-the-thickness thermal conductivities, and consequently C_{HC} has the lowest confidence intervals. Finally, a comparison between C_{eff} and the individual C values is not appropriate because the effective value was calculated using the entire thickness of the OWS, whereas the individual values were calculated with only the top portion. Unlike thermal conductivity, C is a volumetric property, and therefore, C_{eff} represents an averaged value over the entire thickness.

The residuals, computed from the difference between the experimental values and the calculated values with the estimated properties, are shown in Fig. 7. Note, however, that there is a small amount of bias in the solution, especially as the heater is turned off at approximately 2500 min. However, this bias is nonetheless very small (e.g., <0.2 K), and thus the model approximates the actual heating very well.

Detailed Two-Dimensional Model

The in-plane thermal conductivities were estimated using data from six experiments at 295 K using the two-dimensional experimental setup. The average estimates for each temperature and associated 95% confidence intervals calculated from Eqs. (5) and (6) are shown in Table 3. The estimates for $k_{=_{HC}}$ have the smallest confidence intervals, and the sensitivity confidence intervals for the other materials are extremely high. This again is a result of the high sensitivity coefficients for the honeycomb layer relative to the other materials as shown in Fig. 6. This result infers that it is more important to estimate $k_{=_{HC}}$ accurately rather than $k_{=_{CS}}$, $k_{=_{TT}}$, or $k_{=_{FS}}$

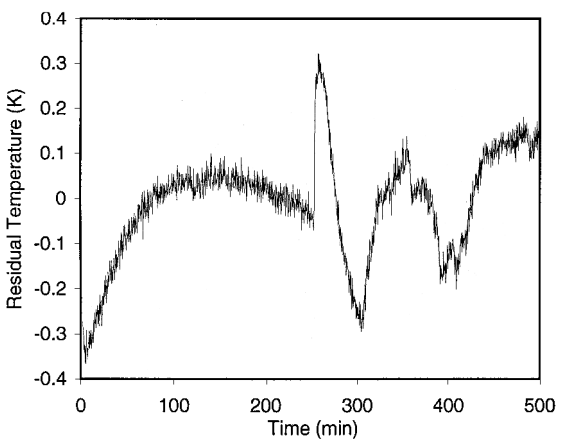

Fig. 7 Temperature residuals from one-dimensional detailed model.

Table 2 Estimates of $k_\perp$ and C for four materials from the one-dimensional detailed model

T, K	$k_{\perp CS}$, W/m · K	$k_{\perp HC}$, W/m · K	$k_{\perp TT}$, W/m · K	$k_{\perp FS}$, W/m · K	C_{CS}, MJ/m^3 · K	C_{HC}, MJ/m^3 · K	C_{TT}, MJ/m^3 · K	C_{FS}, MJ/m^3 · K
295	2.68 ± 130[a]	0.21 ± 2.3[a]	2.34 ± 310[a]	2.04 ± 170[a]	1.22 ± 610[a]	0.75 ± 71[a]	3.00 ± 3700[a]	1.58 ± 1100[a]
	± 2.3[b]	± 0.09[b]	± 2.5[b]	± 4.1[b]	± 1.07[b]	± 0.88[b]	± 5.77[b]	± 1.53[b]
375	0.71 ± 12[a]	0.47 ± 1.7[a]	2.31 ± 100[a]	1.51 ± 43[a]	1.38 ± 190[a]	0.71 ± 23[a]	3.31 ± 1400[a]	1.22 ± 290[a]
	± 1.4[b]	± 0.15[b]	± 1.6[b]	± 1.8[b]	± 0.32[b]	± 0.17[b]	± 1.60[b]	± 0.52[b]
445	1.85 ± 36[a]	0.44 ± 1.9[a]	1.32 ± 68[a]	1.53 ± 51[a]	0.98 ± 190[a]	0.68 ± 25[a]	2.48 ± 1200[a]	3.08 ± 140[a]
	± 1.6[b]	± 0.05[b]	± 0.98[b]	± 2.1[b]	± 0.63[b]	± 0.38[b]	± 0.43[b]	± 1.39[b]

[a] CI_s from Eq. (5). [b] CI_v from Eq. (6).

Table 3 Estimates of $k_=$ for four materials from the two-dimensional detailed model

Temperature, K	$k_=$, W/m · K			
	CS	HC	TT	FS
295	11.8 ± 566[a]	0.20 ± 0.08[a]	20.7 ± 2300[a]	72.8 ± 3640[a]
	± 2.40[b]	± 0.01[b]	± 10.5[b]	± 7.6[b]

[a] CI_s from Eq. (5). [b] CI_v from Eq. (6).

for accurate thermal analyses with this type of heating load, which makes sense because the honeycomb layer not only has a much lower thermal conductivity than the other materials but is also substantially thicker, resulting in a higher resistance to heat transfer in the in-plane direction. Alternately, if higher accuracy in these latter properties is desired, one possibility again is to optimize the experiment through the use of better sensing techniques or the application of a different heating load to provide higher sensitivities.

Convergence of GA

As already discussed, a criterion based on the average of the top 20 objective functions was used to terminate the GA. The number of generations varied from run to run, but on average it took approximately 20 generations for this criterion to be satisfied, with the majority of the changes occurring in the first 10 generations. For each generation the objection function (and therefore the forward problem) is solved for each chromosome in the population; thus, the number of forward problems solved is approximately equal to the number of generations times the elitist population plus the initial population.

Uncertainty of Predicted Temperature

As already noted, the thermal properties are needed for thermal stress analysis, and it is important to determine the effects of the uncertainties in the estimated parameters on the resulting predicted temperature. Based on the analysis by Blackwell et al.,[15] the predicted temperature uncertainty σ_{PT} can be calculated from the uncertainties of each of the parameter estimates as follows:

$$\sigma_{PT}^2 = \sum_{j=1}^{n_p} \left(\frac{\partial T}{\partial \beta_i} s_{\beta_i} \right)^2 \tag{7}$$

where $\partial T / \partial \beta_i$ was calculated from Eq. (4) and s_{β_i} is the same as that calculated for the variance confidence intervals in Eq. (6). Using these values, the one-dimensional detailed model with $n_p = 8$ resulted in a predicted temperature uncertainty σ_{PT} on the order of 10^{-3} K, and the two-dimensional detailed model with with $n_p = 12$ resulted in a predicted temperature uncertainty on the order of 10^{-2} K. Thus, as expected, the high sensitivity confidence intervals did not adversely affect the predicted temperature uncertainties.

Conclusions

A procedure was implemented to estimate the thermal properties of the individual components in a complex aerospace structure. A GA was used to minimize a least-squares function that contained experimental measurements and a mathematical model of the system to estimate simultaneously thermal conductivies and volumetric heat capacities for each of the materials in the structure. A sensitivity study indicated that there was very low sensitivity for many of the properties and that many of the properties were correlated. The use of a nongradient method, such as GAs, allowed for the simultaneous estimation of multiple properties despite these shortcomings.

The low sensitivities of some of the properties resulted in relatively large sensitivity confidence intervals for the resultant estimates because of the small amount of information available for these properties. This result has several implications. First, this indicates that the properties do not need to be known with a high degree of accuracy for the model to be accurate. Second, this might mean that the model could be simplified through, for example, the use of a lumped capacitance model for some of the individual components. Finally, if higher accuracy is needed for these properties, the experimental design might be modified to achieve higher sensitivity.

Finally, the methodology described here is a powerful tool for the characterization of the thermal properties of complex structures. It requires a mathematical model of the structure, experimental measurements with conditions corresponding to the model, and an optimization procedure to obtain the desired properties. The shortcoming of the GA optimization method described here is its inherent slow computation speed (as a result of the number of forward problems that must be solved in the procedure); however, its attributes are that it can handle multiple properties with low sensitivity and high degrees of correlation. Thus, overall, it is a very robust method.

Acknowledgments

This research was funded through a cooperative grant from the NASA Langley Research Center (LaRC) in Hampton, Virginia (Grant NCC-1-221). The authors extend a special thanks to Carl Martin for his help with the finite element code and to all of the support staff at LaRC for their assistance in the experimental efforts.

References

[1] Garcia, S., and Scott, E. P., "Use of Genetic Algorithms in Thermal Property Estimation: Part I—Experimental Design Optimization," *Numerical Heat Transfer*, Vol. 33, No. 2, 1998, pp. 135–147.

[2] Garcia, S., Guynn, J., and Scott, E. P., "Use of Genetic Algorithms in Thermal Property Estimation: Part II—Simultaneous Estimation of Thermal Properties," *Numerical Heat Transfer*, Vol. 33, No. 2, 1998, pp. 149–168.

[3] Parker, W. J., Jemkins, R. J., Butler, C. P., and Abbott, G. L., "Flash Method of Determining Thermal Diffusivity, Heat Capacity, and Thermal Conductivity," *Journal of Applied Physics*, Vol. 32, No. 9, 1961, pp. 1679–1684.

[4] Fukai, J., Nogami, H., Miura, T., and Ohtani, S., "Simultaneous Estimation of Thermophysical Properties by Periodic Hot-Wire Heating Method," *Experimental Thermal and Fluid Science*, Vol. 4, No. 2, 1991, pp. 198–204.

[5] Pilling, M. W., Yates, B., Black, M. A., and Tattersall, P., "The Thermal Conductivity of Carbon Fiber-Reinforced Composites," *Journal of Materials Science*, Vol. 14, No. 6, 1979, pp. 1326–1338.

[6] Beck, J. V., "Transient Determination of Thermal Properties," *Nuclear Engineering Design*, Vol. 3, Nos. 1–3, 1966, pp. 373–381.

[7] Scott, E. P., and Beck, J. V., "Estimation of Thermal Properties in Epoxy Matrix/Carbon Fiber Composite Materials," *Journal of Composite Materials*, Vol. 26, No. 1, 1992, pp. 20–36.

[8] Dowding, K. J., Beck, J. V., Ulbrich, A., and Hayes, J., "Estimation of Thermal Properties and Surface Heat Flux in Carbon-Carbon Composites," *Journal of Thermophysics and Heat Transfer*, Vol. 9, No. 2, 1995, pp. 345–351.

[9]Dowding, K. J., Beck, J. V., and Blackwell, B. F., "Estimation of Directional-Dependent Thermal Properties in a Carbon-Carbon Composites," *International Journal of Heat and Mass Transfer*, Vol. 39, No. 15, 1996, pp. 3157–3164.

[10]Copenhaver, D. C., Scott, E. P., and Hanuska, A., "Thermal Characterization of Honeycomb Sandwich Structures," *Journal of Spacecraft and Rockets*, Vol. 35, No. 4, 1998, pp. 539–545.

[11]Raudensky, M., Woodbury, K., Kral, J., and Brezina, T., "Genetic Algorithm in Solution of Inverse Heat Conduction Problems," *Journal of Numerical Heat Transfer, Part B*, Vol. 28, No. 3, 1995, pp. 293–306.

[12]Fabbri, G., "A Genetic Algorithm for Fin Profile Optimization," *International Journal of Heat and Mass Transfer*, Vol. 40, No. 9, 1997, pp. 2165–2172.

[13]Whetstone, D. W., *Engineering Analysis Language*, Engineering Information Systems, Inc., San Jose, CA, 1983.

[14]Moffat, R. J., "Describing the Uncertainties in Experimental Results," *Experimental Thermal and Fluid Science*, Vol. 1, No. 1, 1988, pp. 3–17.

[15]Blackwell, B. F., Dowding, K. J., Cochran, R. J., and Dobranich, D., "Utilization of Sensitivity Coefficients to Guide the Design of a Thermal Battery," *Proceedings of the ASME Heat Transfer Division*, HTD-Vol. 361-5, American Society of Mechanical Engineers, New York, 1998, pp. 73–82.